AD-A153 651 ON THE ORIGIN OF STREAMWISE VORTICES IN A TURBULENT BOUNDARY LAYER(U) DYNAMICS TECHNOLOGY INC TORRANCE CA P S JANG ET AL. MAR 85 DT-8154-06 N00014-81-C-0440 1/1

UNCLASSIFIED F/G 20/4 NL

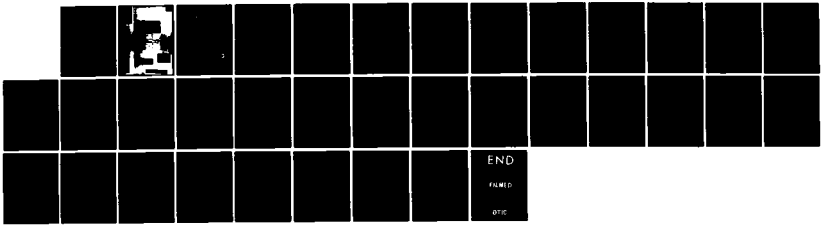

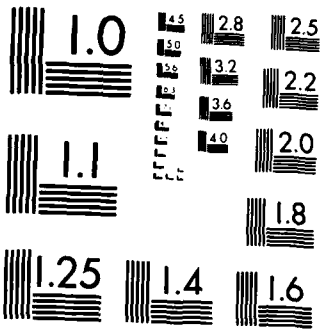

(2)

ON THE ORIGIN OF STREAMWISE VORTICES IN A TURBULENT BOUNDARY LAYER

Dynamics Technology, Inc.

DT-8154-06

ON THE ORIGIN OF
STREAMWISE VORTICES IN
A TURBULENT BOUNDARY LAYER

By: P. S. Jang, D. J. Benney, R. L. Gran

March 1985

Dynamics Technology, Inc.
21311 Hawthorne Blvd., Suite 300
Torrance, California 90503
(213) 543-5433

This work has undergone an extensive internal review before release, both for technical and non-technical content, by an independent review committee.

Project Manager:

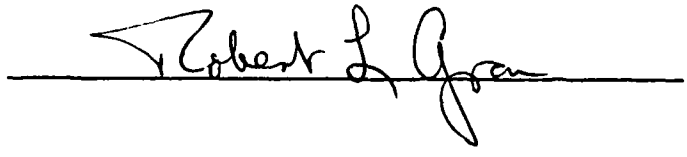

Internal Review:

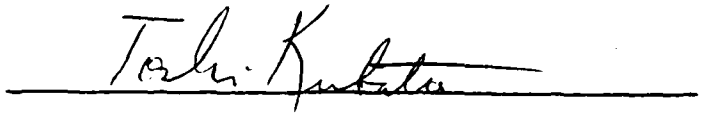

UNCLASSIFIED

SECURITY CLASSIFICATION OF THIS PAGE (When Data Entered)

REPORT DOCUMENTATION PAGE		READ INSTRUCTIONS BEFORE COMPLETING FORM
1. REPORT NUMBER	2. GOVT ACCESSION NO.	3. RECIPIENT'S CATALOG NUMBER
4. TITLE (and Subtitle) On the Origin of Streamwise Vortices in a Turbulent Boundary Layer		5. TYPE OF REPORT & PERIOD COVERED Final Report Nov. 1984 thru No. 1985
		6. PERFORMING ORG. REPORT NUMBER DT-8154-06
7. AUTHOR(s) P. S. Jang, D. J. Benney and R. L. Gran		8. CONTRACT OR GRANT NUMBER(s) N00014-81-C-0440
9. PERFORMING ORGANIZATION NAME AND ADDRESS Dynamics Technology, Inc. 21311 Hawthorne Blvd., Suite 300 Torrance, California 90503		10. PROGRAM ELEMENT, PROJECT, TASK AREA & WORK UNIT NUMBERS
11. CONTROLLING OFFICE NAME AND ADDRESS Office of Naval Research 800 N. Quincy Arlington, VA 22217		12. REPORT DATE March 1985 13. NUMBER OF PAGES 26
14. MONITORING AGENCY NAME & ADDRESS(if different from Controlling Office)		15. SECURITY CLASS. (of this report) UNCLASSIFIED 15a. DECLASSIFICATION/DOWNGRADING SCHEDULE N/A

16. DISTRIBUTION STATEMENT (of this Report)

Unlimited

DISTRIBUTION STATEMENT A
Approved for public release
Distribution Unlimited

17. DISTRIBUTION STATEMENT (of the abstract entered in Block 20, if different from Report)

18. SUPPLEMENTARY NOTES

This research was sponsored under the Compliant Coating Drag Reduction Program at ONR. The Technical Monitor at ONR is Dr. M. Reischman.

19. KEY WORDS (Continue on reverse side if necessary and identify by block number)

Turbulent Boundary Layer; Streamwise Vortices; Low-Speed Streaks; Tollmien-Schlichting Waves; vertical vorticity; Resonant interaction, Weakly non-linear induced flow

20. ABSTRACT (Continue on reverse side if necessary and identify by block number)

Several experiments have suggested that the streamwise vortices, with their accompanying low momentum streaks, in a turbulent boundary layer have a characteristic spanwise wavelength of approximately $\lambda_z^+ = 100$. A mechanism is proposed which selects a comparable spanwise wavelength and produces counter-rotating streamwise vortices in a turbulent boundary layer. Examining the equations which describe the small deviation of the velocity field from its

DD FORM 1 JAN 73 1473 EDITION OF 1 NOV 65 IS OBSOLETE
S/N 0102-LF-014-6601

UNCLASSIFIED

SECURITY CLASSIFICATION OF THIS PAGE (When Data Entered)

20. ABSTRACT (Continued)

time-average, it is found that the Benney-Gustavsson resonance (Studies in Applied Mathematics 3, 1981) occurs with such a boundary layer velocity profile. It is shown that, as an integral part of this resonance, there is a mean secondary flow which has a spanwise wavelength $\lambda_z^+ = 90$ and whose velocities exhibit a counter-rotating streamwise vortex structure.

ABSTRACT

Several experiments have suggested that the streamwise vortices, with their accompanying low momentum streaks, in a turbulent boundary layer have a characteristic spanwise wavelength of approximately $\lambda_z^+ = 100$. A mechanism is proposed which selects a comparable spanwise wavelength and produces counter-rotating streamwise vortices in a turbulent boundary layer. Examining the equations which describe the small deviation of the velocity field from its time-average, it is found that the Benney-Gustavsson resonance (Studies in Applied Mathematics 3, 1981) occurs with such a boundary layer velocity profile. It is shown that, as an integral part of this resonance, there is a mean secondary flow which has a spanwise wavelength $\lambda_z^+ = 90$ and whose velocities exhibit a counter-rotating streamwise vortex structure.

ACKNOWLEDGEMENT

This research was sponsored by the Office of Naval Research under Contract N00014-81-C-0440. The technical monitors for this research are Drs. M. Reischman (at ONR) and J. Hanson (at NRL). The authors gratefully acknowledge the many valuable suggestions and comments of T. Kubota and Y. M. Chen, as well as M. Reischman and J. Hanson. We also thank Y. M. Chen and M. Goforth for their assistance in the numerical computations.

TABLE OF CONTENTS

1. INTRODUCTION

During the last decade, much of the research in turbulent boundary layers has been concerned with the coherent eddy structures that have been observed near the rigid boundary. The quasi-deterministic, randomly-located sequence of coherent structures, collectively called the bursting process, is believed to play a dominant role in the production and maintenance of turbulent flow (for a review, see Cantwell [1]).

One important aspect of the bursting process is believed, by many investigators, to be the counter-rotating streamwise vortex structure with its accompanying low-speed streaks (for example, see Blackwelder [2]). From the many measurements of these streaks, it has been found that the mean streak spacing is approximately 100 $\nu\sqrt{\rho/\tau_w}$, where ν is the kinematic viscosity, ρ is the density and τ_w is the shear stress at the wall. From flow visualizations [3], these low-speed streaks are usually observed to end by being lifted away from the wall. As they are lifted, the streaks start to oscillate with increasing amplitude leading to what is called breakdown. Corino and Brodkey [4] showed that, soon after this breakdown, a large scale motion emanating from the outer flowfield approaches the wall and "cleans" the entire region of the chaotic motion. This phase of the bursting process has been called the sweep.

In experiments using hot-wire anemometers, the bursting process is most easily characterized by a sharp acceleration or the streamwise velocity as reported by Wallace et al. [5] and Blackwelder and Kaplan [6]. To single out the bursting process from the chaotic turbulent motions, Blackwelder and Kaplan used a burst detection technique which relies on this feature of the bursting process. From conditional ensemble averages of data taken in such a way, Blackwelder suggested that the sharp acceleration is the transition between the low-speed streak and the sweep.

Recently, Blackwelder emphasized the similarity between the turbulent boundary layer bursting process and the transition problem [7]. In particular, he found that the conditionally averaged streamwise velocity profile is highly inflectional at and before the burst detection. He further speculated that a

localized shear layer instability might play a role as in the transition problem. The spatial scale of the oscillation of the lifted streak observed in flow visualizations was noted to be consistent with such an interpretation. In any case, in Blackwelder's model, the counter-rotating streamwise vortex pair plays several important roles. The low-speed streaks are attributed to the vortex pair's 'pumping' action of the low speed fluid away from the wall. In turn, the low-speed region is responsible (at least partially) for the inflectional velocity profile which eventually leads to breakdown through a shear-layer instability mechanism.

The aforementioned similarity between the bursting process and the transition problem has suggested to some that the streamwise vortices observed in either case might be due to the same mechanism. In this vein, Coles [8] speculated that the streamwise vortices in a turbulent boundary layer might be the result of a Taylor-Görtler type instability in which the concave flow is due to the large scale motion in the outer flowfield. This idea predicts a spanwise wavenumber for the vortex structure consistent with experiment [2]. However, it appears difficult to justify the extention of the steady state Taylor-Görtler stability analysis to the unsteady flowfield near the flat wall.

Benney and Lin [9,10] proposed another mechanism which attributes the vortex structure in the transitional flow to the secondary mean flow induced by the nonlinear interaction of a two and a three-dimensional wave. Although this mechanism reproduced the essential features of Klebanoff's experiment [11], it has been subject to some criticism. One of the weak points of this theory is that the spanwise wavenumber of the three dimensional wave was chosen to fit the experimental data rather than being predicted (see Stuart [12]).

The purpose of this paper is to follow a somewhat different approach to the cause for streamwise vortices in a turbulent boundary layer. The present hypothesis stems from what is known as the Benney-Gustavsson resonance [13] in which a three-dimensional disturbance with certain wavenumbers can grow to a relatively large amplitude. Benney and Gustavsson showed that there exist exact resonances in various linearized laminar stability problems. However, they found that the resonance condition is only approximately satisfied for

the case of Blausius flow. The effects of the resonance to the transition problem is thus obscured by the existence of an unstable Tollmien-Schlichting wave and the fact that the resonance is only 'close'.

The turbulent pipe flow experiment by Morrison and Kronauer [14] indicates that the statistically dominant streamwise fluctuations have a wavelike character. Further, it appears that a linear or weakly nonlinear perturbation analysis around the mean velocity might be applicable to the turbulent boundary layer problem. Along this line, Landahl [15] and, subsequently, Bark [16], examined the implications of the linear theory with given source terms coming from an assumed model for the Reynolds stress. A particularly interesting result is that Bark's computed energy spectrum for the streamwise velocity fluctuations displays preferred scales in the spanwise and streamwise directions and in time which are in good agreement with Morrison and Kronauer's measurements. However, the bandwidth of the computed spectrum is a few orders of magnitude smaller than was observed experimentally.

Bark attributed the sharpness of his computed spectrum to the crudeness of his model for the Reynold's stress. However, his extremely sharp spectral peak suggests other possibilities such as some sort of resonance. Bark's method of solving the linearized equation for the vertical vorticity implicitly assumed that there is no resonance such as suggested by Benney and Gustavsson. This raises an interesting possibility that the Benney-Gustavsson resonance becomes exact if one replaces the Blasius profile with turbulent boundary layer profile. By examining the eigenvalues of the Orr-Sommerfeld problem and the vertical vorticity equation, this was found to be the case. Details will be discussed in Section 2. Since this resonance becomes exact and since there is no unstable mode for the mean velocity profile, the effects of the resonance could be more pronounced than for the case of the transition problem. Furthermore, the existence of this resonance seems to explain the observed scales of Morrison and Kronauer's experiment and the extreme sharpness of Bark's computed spectral peak.

ith this explanation for the preferred scales of the 3-dimensional disturb-
ıces, we then examine the effects of the nonlinear interaction on this reso-
ınt fundamental mode using the weakly nonlinear perturbation technique. It is
hown in Section 3 that, as an integral part of this resonance, there is a
ean secondary flow which has a spanwise wavelength 90 $\nu\sqrt{\rho/\tau_w}$ and whose
elocities exhibit a counter-rotating streamwise vortex structure. Further
iscussions are made in Section 4.

n Figure 7, the y-dependence of the computed vortex structure with accompany-ng low speed streaks is compared with the vortex structure determined with im's numerical simulation [17]. Only the shape of the vortex structure is ompared since the absolute values are not available in our analysis and the elative strengths of $\langle V \rangle_{max}$ and $\langle U \rangle_{max}$ are not available in Kim's paper. The imilarity of our computed vortex shape with Kim's simulation supports the elevance of the resonance mechanism to the bursting phenomena. The agreement etween Kim's simulation results and Blackwelder and Kaplan's experimental esults is generally good if the slight differences are attributed to differ-nces between temporal and spatial averaging.

To summarize, the induced mean flow is given by

$$\begin{pmatrix} U_M \\ V_M \\ W_M \end{pmatrix} = \begin{pmatrix} \hat{U}_M(y,t)\ \cos(2\beta_o z) \\ \hat{V}_M(y,t)\ \cos(2\beta_o z) \\ -(2\beta)^{-1}\ \partial\hat{V}_M/\partial y\ \sin(2\beta_o z) \end{pmatrix} \tag{3.22}$$

where $\hat{U}_M$ is related to N_M by

$$\hat{U}_M = -\ N_M/2\beta_o\ . \tag{3.23}$$

The y-t dependence of $\hat{U}_M$ is plotted in the first part of Figure 5. As for the vertical component of the induced mean flow, the y-dependence of $\hat{U}_M$ is rather independent of time. The amplitude of $\hat{U}_M$ reaches its maximum value at $t^+ \approx 150$ and then decays very slowly with time. In order to interpret the results plotted in Figure 5, it is helpful to plot the projection, on the (y,z)-plane, of the streamlines. Figure 6 shows the streamline pattern at $t^+ = 40$. Actually, since the y-dependence of $\hat{V}_M$ does not change very much with time either, the streamline pattern is about the same for all time. The streamline pattern clearly shows the counter-rotating longitudinal vortex structure of the induced mean flow. The spanwise wavelength, λ_z^+, of the induced mean flow is 90 which compares favorably with the experimental value of 100.

At $z^+ = 0$, the counter-rotating vortices pump the low-speed fluid up away from the wall so that the streamwise component of the induced mean flow would show a momentum defect. These low-speed streaks would occur every 90 wall units in the spanwise direction.

The function $V_{11}(t,y)$ is then computed by taking the inverse Laplace transform where the integration contour in the complex s-plane should lie below all the poles and the branch cut of the integrand. Note that the pole associated with the source term is located on the branch cut since $R_* > 2\beta_0^2/|\omega_I|$. Further, the singularities in the expressions for the coefficients $A_\pm$, etc., are removable. Therefore, the contour can be deformed to a branch cut integral. For the integration along the branch cut and for the integration over y_0, we have to rely on numerical evaluation. Figure 5 (the second plot) shows the results. Note that the y-dependence of $V_{11}(y,t)$ does not change very much with time. The amplitude of V_{11} reaches its maximum value at $t^+ \equiv tu_\tau^2/\nu \approx 40$ and then decays very slowly compared to the source term's decay rate. (Recall that the source term of equation (3.13) decays as $\exp(-0.074\ t^+)$; in contrast, the value of V_{11} at $t^+ = 200$ is still about 1/3 of its peak.)

To obtain the horizontal components of the induced mean flow, equation (3.5) is examined up to the order of $\varepsilon^{1/2}$. Using equation (3.10) for $U^{(0)}$ and $W^{(0)}$, and equation (3.12) for $V^{(0)}$, the equation for $N^{(1/2)}$ can be simplified to

$$\left[\left(\frac{\partial}{\partial t} + \bar{u}\,\frac{\partial}{\partial x}\right) - \frac{1}{R_*}\,\Delta\right] N^{(1/2)} = 2\beta_o\,\bar{u}'\,V_{11}\,\sin(2\beta_0 z) \tag{3.20}$$

As for the computation for V_{11}, a solution is sought of the form

$$N^{(1/2)} = N_{11}(y,t)\,\sin(2\beta_0 z)\ . \tag{3.21}$$

The resulting equation for $N_{11}(y,t)$ is solved again as an initial value problem assuming that N_{11} vanishes initially. Using the Laplace transform and the Green's function technique, the computation of N_{11} can also be reduced to an evaluation of an integral over y_0 and over a contour in the frequency domain. Once N_{11} is computed, the horizontal components of the induced mean flow are obtained using the continuity equation and the definition of the vertical vorticity.

To obtain a solution $V_M(y,t)$ of equation (3.13), which vanishes at $y = \infty$, we solve equation (3.13) as an initial value problem without assuming the exponential time dependence. Since it is not clear which initial condition for $V_M(y,t)$ is an appropriate one, we shall assume that it vanishes initially and examine the y and t dependences of the resulting solution.

In order to solve the initial value problem, the Laplace transform of equation (3.13) is taken to give

$$\left[is\left(\frac{\partial^2}{\partial y^2} - 4\beta_o^2\right) - \frac{1}{R_*}\left(\frac{\partial^2}{\partial y^2} - 4\beta_o^2\right)^2\right] \tilde{V}_M = -4\, BB^* \frac{\alpha_o^2\beta_o^2}{(\alpha_o^2+\beta_o^2)^2} \frac{\partial(n_o n_o^*)}{\partial y} \frac{1}{2\omega_I - is} \qquad (3.17)$$

where $\tilde{V}_M$ is the Laplace transform of V_M defined as

$$\tilde{V}_M(y,s) = \int_0^\infty dt\, e^{-ist} V_M(y,t) \,. \qquad (3.18)$$

The above equation for $\tilde{V}_M$ is solved using the Green's function technique. The Green's function takes the following form,

$$G = \begin{cases} A_+ e^{-(4\beta_o^2+iRs)^{1/2}(y-y_o)} + B_+ e^{-2\beta_o(y-y_o)} & \text{for } y > y_o \\ A_- e^{-(4\beta_o^2+iRs)^{1/2}(y-y_o)} + B_- e^{-2\beta_o(y-y_o)} + C_- e^{(4\beta_o^2+iRs)^{1/2}(y-y_o)} + D_- e^{2\beta_o(y-y_o)} & \text{for } y < y_o \end{cases} \qquad (3.19)$$

where y_o denotes the support of the delta function, and the coefficients $A_\pm$, $B_\pm$, C_- and D_- are determined from the boundary condition at the wall and the continuity of G, G', G" and the jump condition on G''' at $y = y_o$. Since $\tilde{V}_M$ does not have a homogeneous solution, the Green's function is uniquely defined by these conditions. The branch cut associated with the square root is chosen as in Figure 4.

where ω_I is the imaginary part of ω_o. The function $V_{02}(y)$ is determined from

$$\left[(-2i\omega_o+2i\alpha_o\bar{u})\left(\frac{\partial^2}{\partial y^2}-4\alpha_o^2\right)-2i\alpha_o\bar{u}''-\frac{1}{R_*}\left(\frac{\partial^2}{\partial y^2}-4\alpha_o^2\right)^2\right] V_{02}$$

$$= -2B^2\,\frac{\alpha_o^2\beta_o^2}{(\alpha_o^2+\beta_o^2)^2}\,\frac{\partial(\hat{n}_o\hat{n}_o)}{\partial y} \tag{3.14}$$

As long as $(2\omega_o)$ is not an eigenfrequency of the O-S problem for the case of $\alpha = 2\alpha_o$ and $\beta = 0$, the above equation for V_{02} has a solution.

However, the equation for the induced mean flow requires special treatment. Although the source term in the equation for V_{11} decays with time as $\exp(2\omega_I t)$, the solution V_{11} cannot have the same time dependence. To illustrate this fact, we first assume that V_{11} has the same exponential time-dependence. Then, equation (3.13) reduces to

$$\left[2\omega_I\left(\frac{\partial^2}{\partial y^2}-4\beta_o^2\right)-\frac{1}{R_*}\left(\frac{\partial^2}{\partial y^2}-4\beta_o^2\right)^2\right]\hat{V}_{11} = 4\,BB^*\,\frac{\alpha^2\beta^2}{(\alpha_o^2+\beta_o^2)^2}\,\frac{\partial(\hat{n}_o\hat{n}_o^*)}{\partial y} \tag{3.15}$$

where $\hat{V}_{11}$ is defined by $V_{11} = \hat{V}_{11}(y)\exp(2\omega_I t)$. For simplicity of argument, we assume that the right-hand side of the above equation vanishes for large values of y. The asymptotic solution for $\hat{V}_{11}$ will then be of the form,

$$\hat{V}_{11} = a\,e^{-2\beta_o y} + b\,e^{-\left(4\beta_o^2+2\omega_I R_*\right)^{1/2} y} \tag{3.16}$$

If $(2\omega_I R_* + 4\beta_o^2)$ were positive, then the sign of the square root could be chosen to be positive so that $\hat{V}_{11}$ would vanish at infinity. However, the argument of the square root at the resonant point is negative.

where α_o and β_o are the wavenumbers at the direct resonance. Using the continuity equation and the definition of N, $U^{(0)}$ and $W^{(0)}$ can be obtained from $N^{(0)}$ as

$$\begin{Bmatrix} U^{(0)} \\ W^{(0)} \end{Bmatrix} = B \begin{Bmatrix} -\frac{\beta_o \hat{n}_o}{\alpha_o^2+\beta_o^2} \cos\beta_o z \\ \frac{i\alpha_o \hat{n}_o}{\alpha_o^2+\beta_o^2} \sin\beta_o z \end{Bmatrix} e^{i\alpha_o x - i\omega_o t} + (\ * \ ) \qquad (3.10)$$

The equation for $V^{(0)}$ is obtained from equation (3.4);

$$\{(\frac{\partial}{\partial t} + \bar{u}\frac{\partial}{\partial x})\Delta - \bar{u}''\frac{\partial}{\partial x} - \frac{1}{R_*}\Delta^2\} V^{(0)} = \frac{\partial^3}{\partial x^2 \partial y}(U^{(0)}U^{(0)})$$

$$+ 2\frac{\partial^3}{\partial x \partial z \partial y}(U^{(0)}W^{(0)}) + \frac{\partial^3}{\partial z^2 \partial y}(W^{(0)}W^{(0)}) . \qquad (3.11)$$

The time averages of $U^{(0)}U^{(0)}$ and $W^{(0)}W^{(0)}$ are dropped since $U^{(0)}$ and $W^{(0)}$ decay exponentially with time.

An examination of the source terms shows that the particular solution for $V^{(0)}$ is of the form

$$V^{(0)} = V_M(y,t)\cos(2\beta_o z) + (V_{02}(y)\, e^{2i\alpha_o x - 2i\omega_o t} + \ * \ ) \qquad (3.12)$$

We will refer to the first term as the induced mean flow and the second term as the induced second harmonic. The function $V_M(y,t)$ is determined as a solution of the following equation

$$[\frac{\partial}{\partial t}(\frac{\partial^2}{\partial y^2} - 4\beta_o^2) - \frac{1}{R_*}(\frac{\partial^2}{\partial y^2} - 4\beta_o^2)^2] V_M = 4\, BB^* \frac{\alpha_o^2\beta_o^2}{(\alpha_o^2+\beta_o^2)^2} \frac{\partial(\hat{n}_o\hat{n}_o^*)}{\partial y} e^{2\omega_I t} \qquad (3.13)$$

$$\left[\left(\frac{\partial}{\partial t} + \bar{u}\,\frac{\partial}{\partial x}\right) - \frac{1}{R_*}\,\Delta\right] N + \epsilon^{1/2}\left[\bar{u}'\,\frac{\partial U}{\partial z} + \frac{\partial^2}{\partial x \partial z}\left((UU-\overline{UU}) - (WW-\overline{WW})\right)\right.$$

$$\left. + \left(\frac{\partial^2}{\partial z^2} - \frac{\partial^2}{\partial x^2}\right)(UW-\overline{UW})\right]$$

$$+ \epsilon\left[\frac{\partial}{\partial y \partial z}(UV-\overline{UV}) - \frac{\partial^2}{\partial x \partial y}(VW-\overline{VW})\right] = 0 \qquad (3.5)$$

$$\frac{\partial U}{\partial x} + \frac{\partial W}{\partial z} + \epsilon^{1/2}\,\frac{\partial V}{\partial y} = 0 \qquad (3.6)$$

$$N = \frac{\partial U}{\partial z} - \frac{\partial W}{\partial x} \qquad (3.7)$$

Equation (3.5) is linear when $\epsilon = 0$, and a systematic perturbation scheme is readily developed (i.e., $N = N^{(0)} + \epsilon^{1/2} N^{(1/2)} + \ldots$, etc.). The zeroth order term in such an expansion gives

$$N^{(0)} = B\,\hat{\eta}_0(y)\,\sin\beta_0 z\, e^{i\alpha_0 x - i\omega_0 t} + B^*\,\hat{\eta}_0(y)\,\sin\beta_0 z\, e^{-i\alpha_0 x - i\omega_0^* t} \qquad (3.8)$$

where * denotes the complex conjugate. The function $\hat{\eta}_0$ is determined as a solution to the eigenvalue problem

$$\left[i\alpha_0(\bar{u}-c) - \frac{1}{R_*}\left(\frac{\partial^2}{\partial y^2} - \alpha_0^2 - \beta_0^2\right)\right]\hat{\eta}_0 = 0\ ;\quad \hat{\eta}_0(0) = \hat{\eta}_0(\infty) = 0 \qquad (3.9)$$

3. MEAN FLOW INDUCED BY THE RESONATING FUNDAMENTAL MODES

From equations (2.15) and (2.16), it is apparent that if α, β and ω correspond to a direct resonance, then so do α, $-\beta$ and ω. So, there are at least two resonant modes. The nonlinear theoretical consequences of two or more resonant modes were analyzed by Benney and Gustavsson. We shall rely on their formalism to compute the mean flow induced by these resonant modes.

They first observed that equations (2.6) and (2.7) imply that, for the case of two resonant modes, the dominant terms in the higher-order expansion for v and η are of the form

$$v \sim (1 + \varepsilon^2 t^4 + \ldots)\, e^{i\alpha x + i\beta z - i\omega t} \tag{3.1}$$

$$\eta \sim (t + \varepsilon^2 t^5 + \ldots)\, e^{i\alpha x + i\beta z - i\omega t} \tag{3.2}$$

where ε is the nonlinear parameter related to the small amplitude of fluctuation. Thus, they argue, the appropriate time scale is $\varepsilon^{1/2}t$ and the perturbation must be rescaled in the form

$$v = V, \quad (u,w,\eta) = \varepsilon^{-1/2}\,(U,W,N) \tag{3.3}$$

The nonlinear perturbation equations then become

$$\left[\left\{\left(\frac{\partial}{\partial t} + \bar{u}\,\frac{\partial}{\partial x}\right)\Delta - \bar{u}''\,\frac{\partial}{\partial x} - \frac{1}{R_*}\Delta^2\right\} V\right.$$

$$\left. - \frac{\partial^3}{\partial x^2 \partial y}\left(UU - \overline{UU}\right) - 2\,\frac{\partial^3}{\partial x \partial z \partial y}\left(UW - \overline{UW}\right) - \frac{\partial^3}{\partial z^2 \partial y}\left(WW - \overline{WW}\right)\right]$$

$$+ \varepsilon^{1/2}\left[\left(\frac{\partial^2}{\partial x^2} + \frac{\partial^2}{\partial z^2} - \frac{\partial^2}{\partial y^2}\right)\left(\frac{\partial}{\partial x}\left(UV - \overline{UV}\right) + \frac{\partial}{\partial z}\left(WV - \overline{WV}\right)\right)\right]$$

$$+ \quad \varepsilon\left[\left(\frac{\partial^2}{\partial x^2} + \frac{\partial^2}{\partial z^2}\right)\frac{\partial}{\partial y}\left(VV - \overline{VV}\right)\right] = 0 \tag{3.4}$$

density as a function of ω_R and either α or β. Figure 3 shows their contour plots of $\mathcal{P}_u(\alpha^+,\omega_R^+)$ and $\mathcal{P}_u(\beta^+,\omega_R^+)$ where these quantities are related to the power spectrum P_u as

$$\mathcal{P}_u(\alpha^+,\omega^+) = \alpha^+\omega^+ \; P_u(\alpha^+,\omega^+) \tag{2.27}$$

$$\mathcal{P}_u(\beta^+,\omega^+) = \beta^+\omega^+ \; P_u(\beta^+,\omega^+) \tag{2.28}$$

These spectral functions plotted in logarithm scales permit one to make a visual comparison of the relative power in various wavenumber/frequency bands (the power is the contour level times the area as seen in the figure).

The particular spectra measured at $y^+ = 14.8$ were chosen because this location is the closest of their data to the peak of the resonant free mode of the vertical vorticity equation (see Figure 1). The predicted position of the spectral peak based on the direct resonance is denoted by the intersection of the two dashed lines in each spectrum. The prediction is in good agreement with the experimental data.

$$a = \frac{\beta \int \hat{\eta}_F \bar{u}' \hat{v}\, dy}{\int \eta_F \eta_F\, dy} \quad . \quad . \qquad (2.23)$$

We examined whether such a resonance occurs when $\bar{u}$ is taken to be a turbulent boundary layer's mean profile. For this purpose, we have to rely on numerical solutions of the eigenvalue problems associated with equations (2.15) and (2.18). If two eigenvalues coincide, then resonant growth occurs. One such resonance was found when the wavenumbers (expressed in 'wall units'; $\alpha^+ \equiv \alpha\nu/u_\tau$, $\beta^+ \equiv \beta\nu/u_\tau$, where $u_\tau \equiv \sqrt{\tau_w/\rho}$) are

$$\alpha^+ = 0.0093 \qquad (2.24)$$

$$\beta^+ = 0.035 \qquad (2.25)$$

The location of this resonance in this dimensionless wavenumber appears to be independent of the Reynolds number (we examined the Reynolds number dependence for $1000 \leq R_\star \leq 15{,}000$). At this resonant point the eigenfrequencies of the O-S and the V-V equations are the same and given by

$$\omega^+ \equiv \frac{\omega\nu}{u_\tau^2} = 0.090 - i0.037 \qquad (2.26)$$

This resonance was found numerically by locating the intersection of the zero lines of the real and the imaginary parts of $[c(\alpha,\beta;R_\star) - c'(\alpha,\beta;R_\star)]$ in the α-β plane. The boundary layer velocity profile used for these computations incorporated the well-known Law of the Wall and Law of the Wake along with a sublayer "patch" based on van Driest's damping factor. This sublayer patch results in a velocity profile that is in good agreement with experiment over the entire boundary layer. The normal coordinate dependence of the O-S eigenmode and V-V eigenmode are plotted in Figures 1 and 2, respectively.

Because of the potentially large amplitude associated with the secular behavior, the above values of α^+, β^+ and ω_R^+ (real part of ω^+) should correspond to the position of a local peak in the power spectral density of the horizontal velocity. Experimental evidence for the correctness of this prediction can be found in Morrison and Kronauer's experiment [14]. Measuring the fluctuation of the streamwise velocity, they obtained the power spectral

subject to the boundary conditions; $\hat{v} = 0$, $\frac{d\hat{v}}{dy} = 0$, $\hat{\eta} = 0$ at $y = 0, \infty$. Here, c denotes the phase velocity defined by $c = \omega/\alpha$. Equation (2.15) is the Orr-Sommerfeld (O-S) equation, and (2.16) will be referred to as the vertical vorticity (V-V) equation. The O-S eigenvalue problem leads to a set of eigenvalues

$$c = c(\alpha, \beta; R_*) \ . \tag{2.17}$$

The V-V equation is usually solved as a forced response. This approach implicitly assumes that the eigenfrequencies of the O-S equation do not match any of the free mode eigenfrequencies for the V-V equation, that is, the eigenfrequencies of the problem

$$\left[i\alpha(\bar{u}-c) - \frac{1}{R_*}\left(\frac{\partial^2}{\partial y^2} - \alpha^2-\beta^2\right)\right] \hat{\eta}_F = 0 \ ; \ \ \hat{\eta}_F = 0 \ \ \text{at } y = 0, \infty \ . \tag{2.18}$$

Denoting the set of V-V free-mode eigenfrequencies by

$$c' = c'(\alpha,\beta;R_*) \ , \tag{2.19}$$

the condition for direct resonance can be written as

$$c(\alpha,\beta;R_*) = c'(\alpha,\beta;R_*) \ . \tag{2.20}$$

If such a resonant condition is satisfied, the solution to the V-V equation behaves as

$$\eta \sim \text{at } \hat{\eta}_F(y) \ e^{-i\omega t+i\alpha x+i\beta z} \tag{2.21}$$

while

$$v \sim \ \hat{v}(y) \ \ e^{-i\omega t+i\alpha x+i\beta z} \ . \tag{2.22}$$

Note that the secular solution for η initially grows linearly with time so that relatively large horizontal motions might be induced. Here, the parameter 'a' which determines the initial growth rate of the secular term is

$$S_1 = \frac{\partial}{\partial x}\left(uu - \overline{uu}\right) + \frac{\partial}{\partial y}\left(vu - \overline{vu}\right) + \frac{\partial}{\partial z}\left(wu - \overline{wu}\right) \tag{2.8}$$

$$S_2 = \frac{\partial}{\partial x}\left(uv - \overline{uv}\right) + \frac{\partial}{\partial y}\left(vv - \overline{vv}\right) + \frac{\partial}{\partial z}\left(wv - \overline{wv}\right) \tag{2.9}$$

$$S_3 = \frac{\partial}{\partial x}\left(uw - \overline{uw}\right) + \frac{\partial}{\partial y}\left(vw - \overline{vw}\right) + \frac{\partial}{\partial z}\left(ww - \overline{ww}\right) . \tag{2.10}$$

The horizontal components of the velocity perturbation are related to v and η by the equations

$$\frac{\partial u}{\partial x} + \frac{\partial w}{\partial z} = - \frac{\partial v}{\partial y} \tag{2.11}$$

$$\frac{\partial u}{\partial z} - \frac{\partial w}{\partial x} = \eta . \tag{2.12}$$

We next linearize equation (2.3) and seek normal mode solutions of the form

$$v = \hat{v}(y)\ e^{i\alpha x + i\beta z - i\omega t} \tag{2.13}$$

$$\eta = \hat{\eta}(y)\ e^{i\alpha x + i\beta z - i\omega t} \tag{2.14}$$

where α and β are wavenumber components in the streamwise and spanwise direction and ω is the wave's frequency. The following equations are then obtained

$$\left[i\alpha(\bar{u}-c)\left(\frac{\partial^2}{\partial y^2} - \alpha^2-\beta^2\right) - i\alpha\bar{u}'' - \frac{1}{R_*}\left(\frac{\partial^2}{\partial y^2} - \alpha^2-\beta^2\right)\right] \hat{v} = 0 \tag{2.15}$$

$$\left[i\alpha(\bar{u}-c) - \frac{1}{R_*}\left(\frac{\partial^2}{\partial y^2} - \alpha^2-\beta^2\right)\right] \hat{\eta} = - i\beta\bar{u}'\ \hat{v} \tag{2.16}$$

resonance by which disturbances with certain scales can grow, at least momentarily, by subtracting energy from the mean flows. Since the eigenmodes whose peak values are near the turbulent boundary layer's sublayer decay rather rapidly, such a resonance will only be effective if it occure in the lowest possible order of the expansion in order to reverse the energy loss even momentarily.

The direct resonance suggested by Benney and Gustavsson does arise ir the linearized equations of (2.3) and (2.4). Another interesting property of the direct resonance is that at a given Reynolds number, it occurs only at discrete locations in wavenumber space (i.e., only those components with certain combinations of wavelength and obliquity are resonant). Therefore, this resonance seems to be an ideal candidate for a mechanism which allows disturbances with certain scales to be energetically dominant.

To examine the possibility of direct resonance in a turbulent boundary layer, the small disturbance equations are made dimensionless by utilizing the boundary layer's displacement thickness, δ^*, and the freestream velocity $\bar{u}_\infty$. In the non-dimensional form of the equations, we set $\bar{u}_\infty \delta^*/\nu \equiv R_*$. As is customary for the boundary layer problem, x, y and z are taken to denote the streamwise, the normal and the spanwise coordinates, respectively. The velocity components will be denoted by u , v and w. Elimination of the pressure from (2.3) gives

$$\left(\frac{\partial}{\partial t} + \bar{u}\frac{\partial}{\partial x}\right)\Delta v - \bar{u}''\frac{\partial v}{\partial x} + \epsilon\left[\left(\frac{\partial^2}{\partial x^2} + \frac{\partial^2}{\partial y^2}\right)S_2 - \frac{\partial S_1}{\partial x \partial y} - \frac{\partial^2 S_3}{\partial z \partial y}\right] = \frac{1}{R_*}\Delta^2 v \qquad (2.6)$$

$$\left(\frac{\partial}{\partial t} + \bar{u}\frac{\partial}{\partial x}\right)\eta + \bar{u}'\frac{\partial v}{\partial z} + \epsilon\left[\frac{\partial S_1}{\partial z} - \frac{\partial S_3}{\partial x}\right] = \frac{1}{R_*}\Delta\eta \ . \qquad (2.7)$$

Here the prime denotes differentiation with respect to y, and η is the vertical vorticity $\left(\eta = \frac{\partial u}{\partial z} - \frac{\partial w}{\partial x}\right)$. ϵ is a nonlinear parameter related to the small amplitude of the fluctuations, and S_j are defined by

2. DIRECT RESONANCE IN A TURBULENT BOUNDARY LAYER

The velocity and pressure field in a turbulent boundary layer are split into a mean and a fluctuating part according to

$$U_i = \bar{u}_i + u_i \tag{2.1}$$

$$P = \bar{p} + p \tag{2.2}$$

where the overbar denotes the time average. Then, the equations governing the fluctuating part can be obtained by substituting (2.1) and (2.2) into the Navier-Stokes equations and subtracting the mean part;

$$\frac{\partial u_i}{\partial t} + \bar{u}_j \nabla_j u_i + u_j \nabla_j \bar{u}_i = -\frac{1}{\rho} \nabla_i p + \nu \Delta u_i + \nabla_j \left(\overline{u_j u_i} - u_j u_i \right) \tag{2.3}$$

$$\nabla_i u_i = 0 \ . \tag{2.4}$$

Here, ρ is the density of the fluid and ν is the kinematic viscosity, both taken as constant.

The mean flow will be assumed to be parallel such that

$$\bar{u}_i = (\bar{u}(y), 0, 0) \ . \tag{2.5}$$

The mean velocity distribution $\bar{u}(y)$ for the case of a turbulent boundary layer will be considered to be known. The key assumption in our analysis of (2.3) is that the effects of nonlinear terms are important only intermittently. The streamwise vortices and the accompanying low-speed streaks which seem to provide the set-up for a burst are assumed to be weakly nonlinear phenomena.

With these assumptions, equations (2.3) and (2.4) are analyzed using perturbation techniques. It is well known that all the eigenvalues of the linearized equations of (2.3) and (2.4) result in decaying solutions, i.e., all disturbances lose energy to the mean flow. However, there might be a possible

4. CONCLUDING REMARKS

It is natural to be concerned with the robustness of the direct resonance, and the effects on the resonant condition of different boundary conditions, mean profiles, and with eddy viscosity terms in the equation were examined. Including eddy viscosity terms does not affect the existence of a direct resonance and the computed induced mean flow exhibits features similar to those described in Section 3. With the mean profile measured by Reischman and Tiderman [18] for a polymer injected turbulent boundary layer, the direct resonance was still found to remain. The spanwise wavenumber at the resonance is, however, smaller than that for the 'universal' mean profile, which agrees with experimental evidence of the wider streak spacing for a polymer added flow. We also showed that direct resonance should be virtually unaffected even if the rigid wall were replaced with a compliant wall.

As will be discussed, there are, of course, several aspects of the present theory that remain incomplete. However, this study provides strong evidence for the relevance of direct resonance to the streamwise vortices observed in a turbulent boundary layer. In terms of the energy exchange between the mean flow and the fluctuations, direct resonance can be interpreted as follows: the source term in the linearized vertical vorticity equation (2.16) reflects the production of horizontal disturbance energy by the action of the mean field, $\bar{u}$, against the uv-component of the Reynold's stresses. When the wavenumbers and the frequency associated with an O-S eigenmode correspond to those of a free mode of the vertical vorticity, the production of energy through the uv-Reynolds stress becomes more efficient. This situation is similar to the harmonic oscillator driven by broadband noise about its natural frequency.

There are two main pieces of evidence for the relevance of such a mechanism to the bursting process. One is that the wavenumbers and frequency at resonance are close to the values associated with the most intense waves measured by Morrison and Kronauer near the sublayer boundary. The other is that the secondary mean flow induced by this resonant fundamental mode contains a streamwise vortex structure. The theoretical shape of the vortices and the spacing of the accompanying low-speed streaks are comparable to experimental findings.

One of the problems which has not been addressed is a comparison of the resonant point and other points in wavenumber space. In order to extend the theory to predict the power spectral distribution, this issue has to be addressed. A difficulty associated with this extension is that although the resonant mode initially grows with time, the exponentially decaying factor eventually dominates and the mode decays. Therefore, without a fresh supply of disturbances, this resonance cannot sustain itself. In this respect, a potentially important property of this resonant mode seems to be the inflectional instability. As a test, we considered a one parameter family of mean profiles which starts with the universal mean profile at s = 0 and ends with the inflectional profile found by Blackwelder and Kaplan [6] at s = 1, (i.e., $u_s(y) = (1-s)\,\bar{u}(y) + s\,u_{BK}$, where u_{BK} denotes the Blackwelder and Kaplan profile). As s increases, the damping factor associated with the Orr-Sommerfeld mode becomes smaller and near s = 0.7 that mode becomes unstable. As it becomes unstable, it can no longer resonate with the vertical vorticity mode since it can be shown analytically that all the free vertical vorticity modes are damped. Although at s = 0 the resonant Orr-Sommerfeld mode is not the least damped mode (actually it is the second least damped mode; the eigenfrequency of the least damped mode being $\omega^+ = 0.13 + i0.035$ at α^+ and β^+ given by equations (2.24) and (2.25)), as s increases this order in damping factor changes and only the resonant mode becomes unstable at s = 1. These two properties of the second mode (when ordered by the imaginary part of the eigenfrequency), i.e., the direct resonance and the inflectional instability, might be the reasons why it plays an important role even if it has a slightly larger damping factor. However, to estimate these effects quantitatively appears to require a more systematic account of the several lowest modes with varying wavenumbers.

Another problem which has not been considered concerns the origin and mathematical description of the sweep. This might involve a very complicated interaction between the outer flow and the near wall flow. In this regard, it seems appropriate to mention that the induced mean flow in Section 3 was represented by an integral along a branch cut in the complex frequency plane. This branch cut is what Mack [19] interpreted as the continuous spectrum. For a frequency in this continuous spectrum, the corresponding eigensolution does

not decay exponentially but becomes oscillatory as y approaches infinity. This raises the possibility that the interaction between the inner and the outer flows could be described through the induced mean flow. Recall that the initial condition for the induced mean flow was chosen to be zero in Section 3 since we do not know what an appropriate condition should be. Perhaps by choosing an initial condition appropriate to a finite wavepacket rather than an infinite plane wave, the time development of the induced mean flow would exhibit characteristics of the sweep in addition to the vortex structure.

REFERENCES

1. Cantwell, B. J., Ann. Rev. Fluid Mech. 13, 457 (1981).

2. Blackwelder, R. F., in Coherent Structures of Turbulent Boundary Layers, (eds. C. R. Smith and D. E. Abbott) p. 211, Lehigh University (1979).

3. Kline, S. J., Reynolds, W. D., Schraub, J. A. and Renstadler, P. W., J. Fluid Mech. 30, 74 (1967).

4. Cornio, E. R. and Brodkey, R. S., J. Fluid Mech. 37, 1 (1969).

5. Wallace, J. W., Brodkey, R. S. and Eckelmann, H., J. Fluid Mech. 83. 673 (1977).

6. Blackwelder, R. F. and Kaplan, R. E., J. Fluid Mech. 76, 89 (1976).

7. Blackwelder, R. F., Phys. Fluid 26, 2807 (1983).

8. Coles, D., in Coherent Structures of Turbulent Boundary Layers, (eds. C. R. Smith and D. E. Abbott) 462, Lehigh University (1979).

9. Benney, D. J., J. Fluid Mech. 10, 209 (1961).

10. Lin, C. C. and Benney, D. J., American Math. Soc., Proceedings of Symposia in Applied Math. 13, 1 (1962).

11. Klebanoff, P. D., Tidstrom, D. and Sargent, L. M., J. Fluid Mech. 12, 1 (1962).

12. Stuart, J. T., J. Fluid Mech. 29, 417 (1967).

13. Benney, D. J. and Gustavsson, L. H., Studies in Appl. Math. 64, 185 (1981).

14. Morrison, W. R. B. and Kronauer, R. E., J. Fluid Mech. 39, 117 (1969).

15. Landahl, M. T., J. Fluid Mech. 29, 441 (1967).

16. Bark, F. H., J. Fluid Mech. 70, 229 (1975).

17. Kim, J., Phys. Fluids 26, 2088 (1983).

18. Reischman, M. M. and Tiderman, W. G., J. Fluid Mech. 70, 369 (1975).

19. Mack, L. M., J. Fluid Mech. 73, 497 (1976).

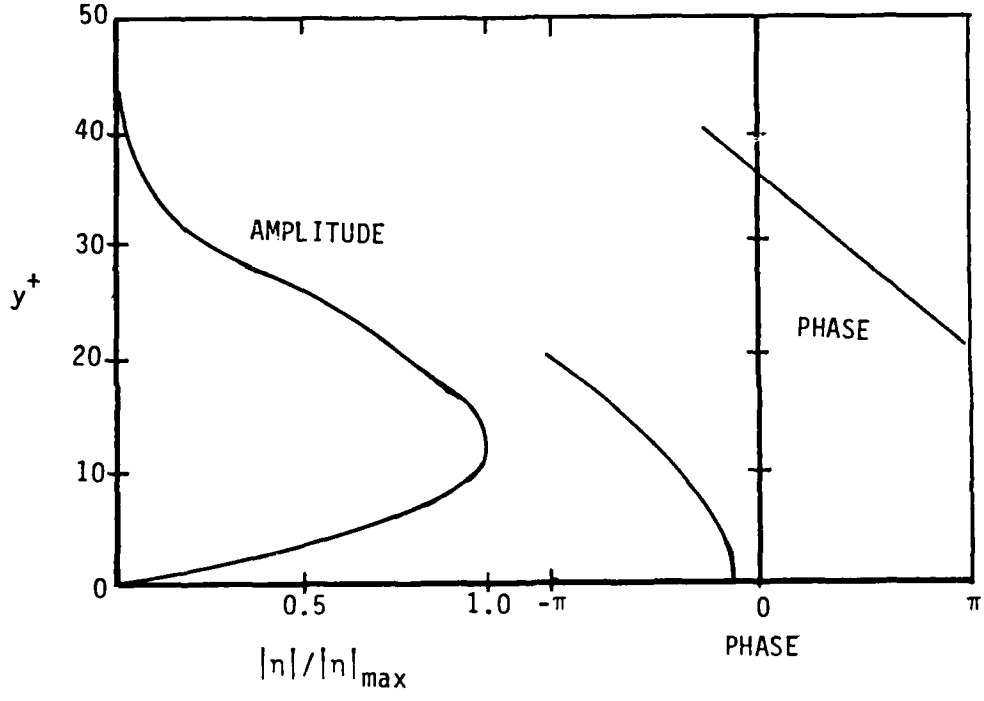

Figure 1. The amplitude and phase distribution of the resonant vertical vorticity mode.

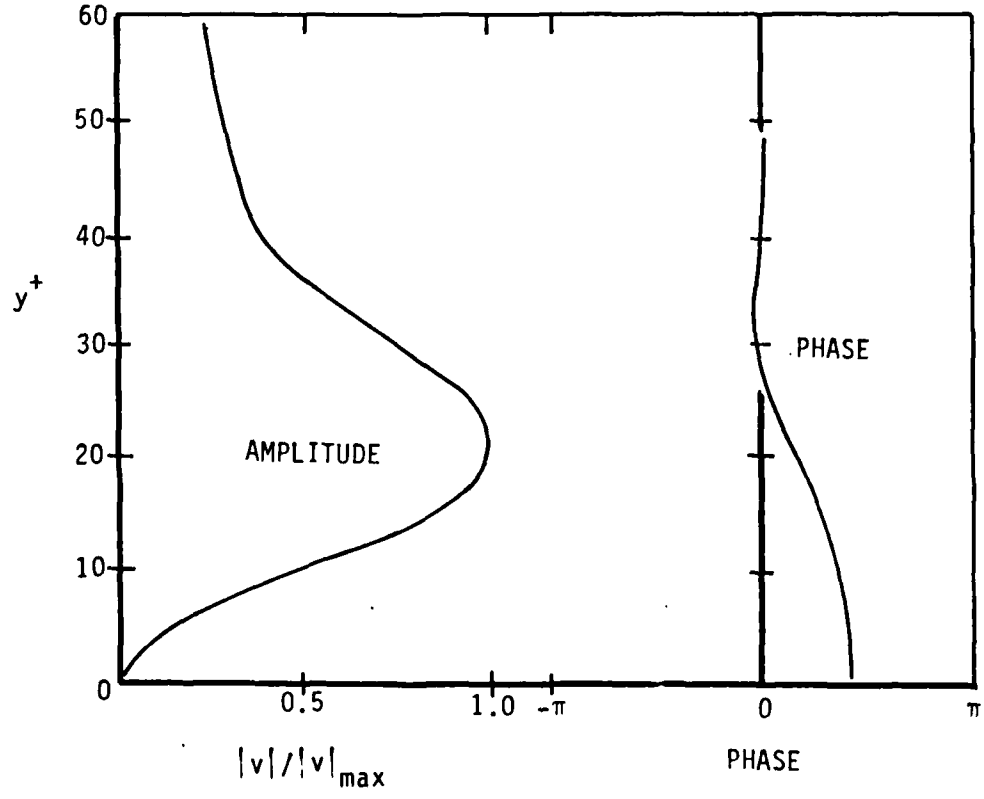

Figure 2. The amplitude and phase distribution of the resonant Orr-Sommerfeld mode.

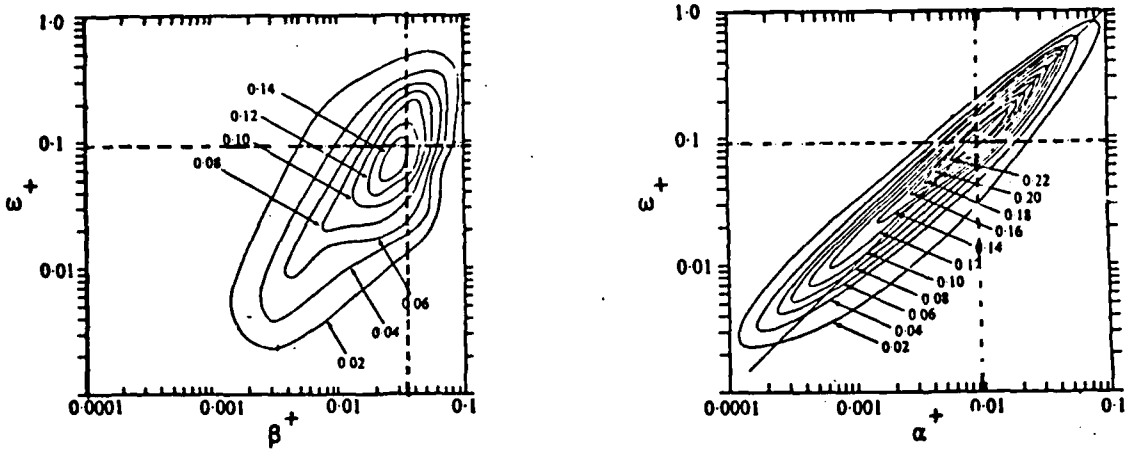

Figure 3. Comparison of the resonant point with the peak position of Morrison and Kronauer's spectrum.

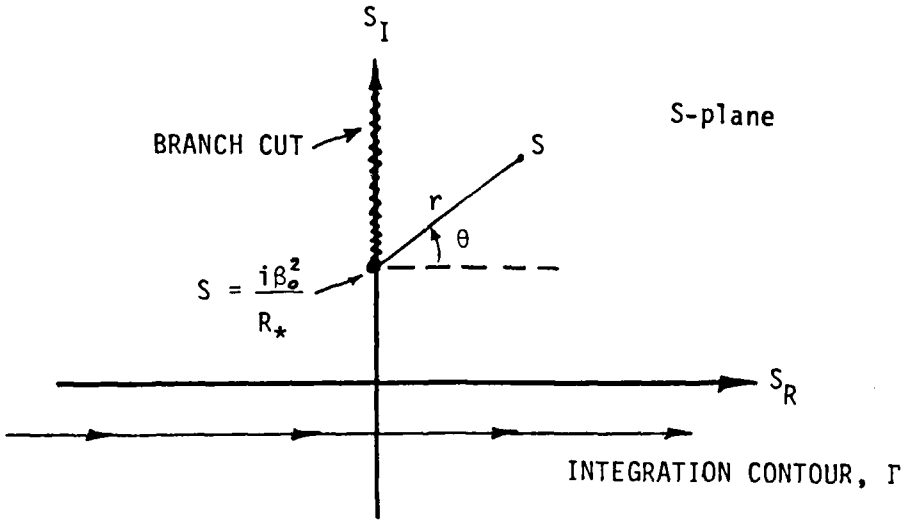

Figure 4. Branch cut of $(4\beta^2 + iRS)^{1/2}$. $(4\beta^2 + iRS)^{1/2}$ is defined by $R^{1/2}\, r \exp i\,(\theta/2 + \pi/4)$ where θ varies from $(-3\pi/2)$ to $(\pi/2)$.

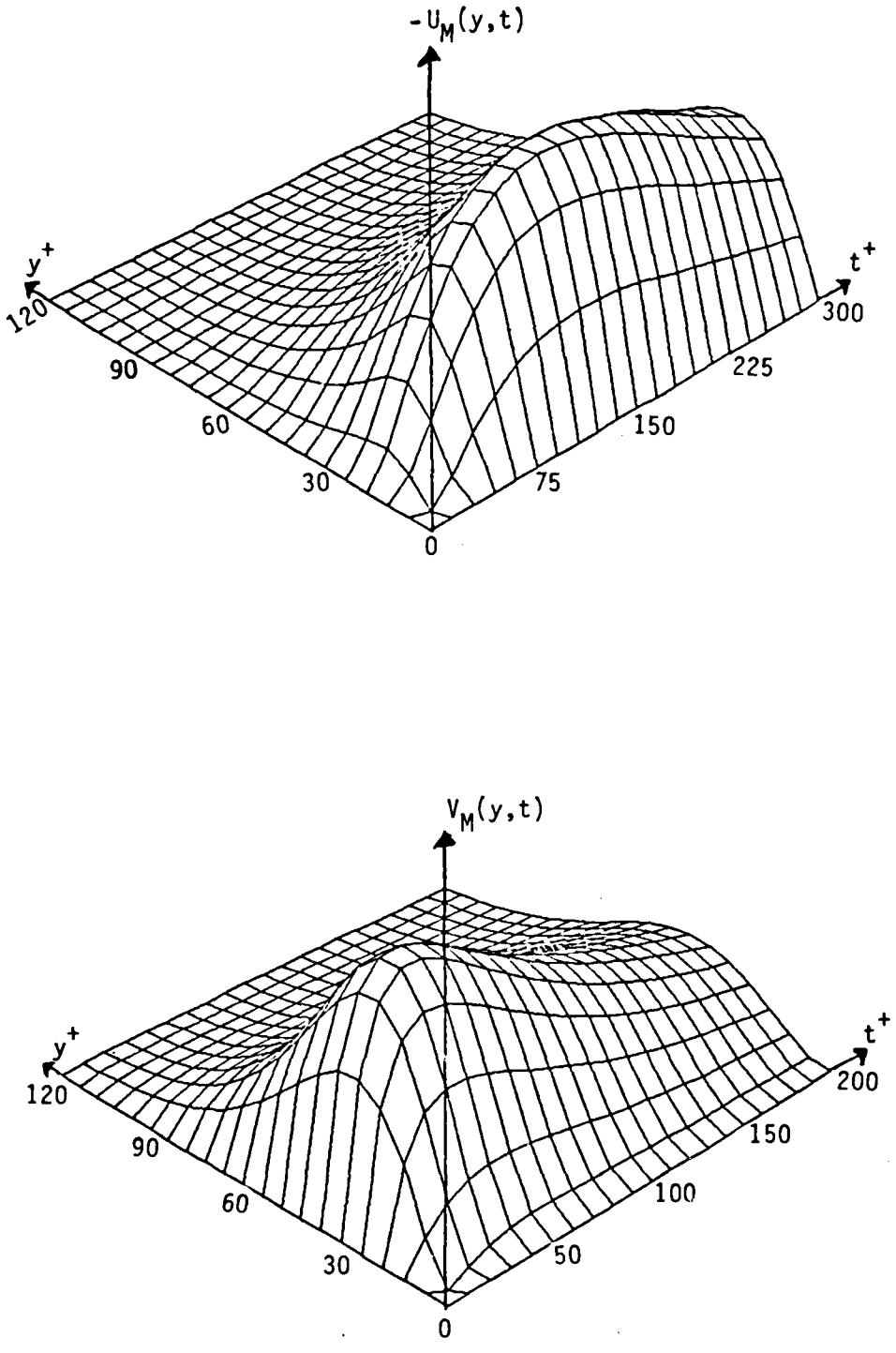

Figure 5. Plots of the vertical and streamwise components of the induced mean flow. The maximum of $|u_M(y,t)|$ is about 43% of the maximum of $v_M(y,t)$.

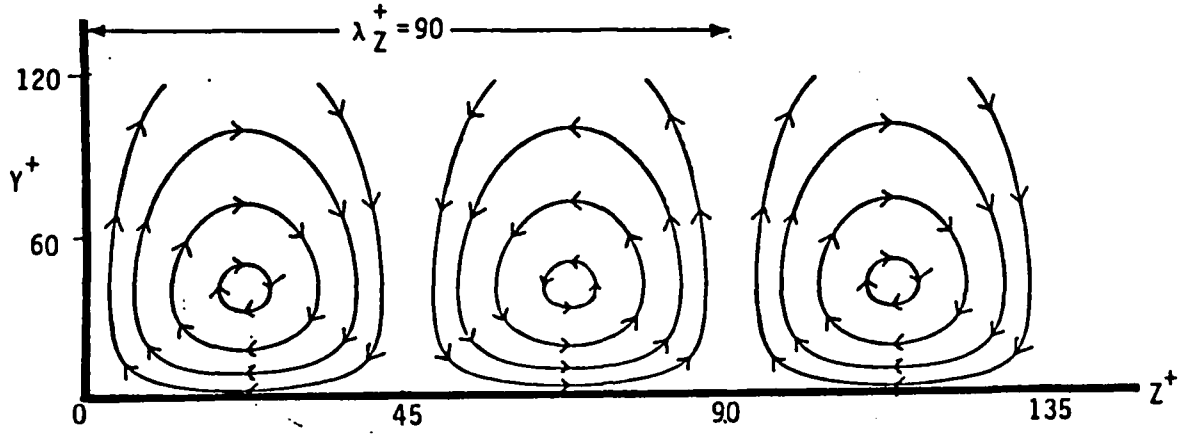

Figure 6. Computed streamline pattern of the induced mean flow at $t^+ = 40$. This pattern does not change for other values of t^+ as can be inferred from Figure 5.

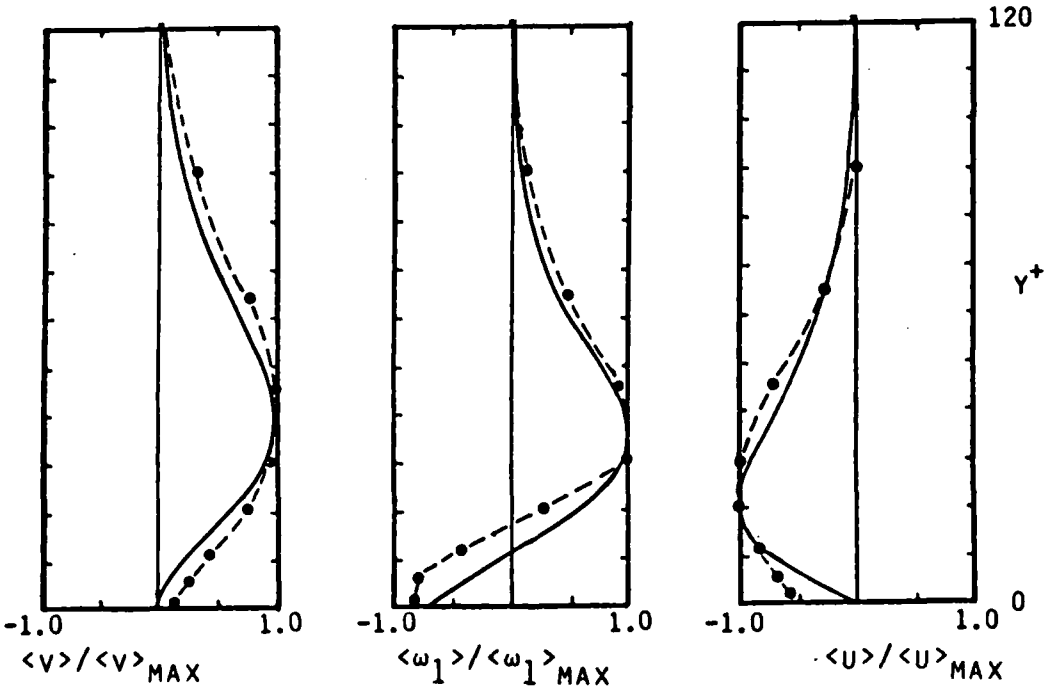

Figure 7. Comparison of the computed vortex structure with that of Kim [9]. The solid lines represent the analysis result and the dots connected with the dashed lines represent Kim's result at $X^+ = 125$, where $X^+ = 0$ corresponds to the burst detection point. ω_1 denotes the streamwise vorticity.

END

FILMED

6-85

DTIC